JOC The Journal of Organic Chemistry

Article

pubs.acs.org/joc

Synthesis and Investigation of the Effect of Substitution on the Structure, Physical Properties, and Electrochemical Properties of Anthracenodifuran Derivatives

Motonori Watanabe,*[,†] Yasutaka Doi,[‡] Hidehisa Hagiwara,[†,§] Aleksandar Tsekov Staykov,[†] Shintaro Ida,[†,§] Taisuke Matsumoto,[∥] Teruo Shinmyozu,[∥] and Tatsumi Ishihara*[,†,‡,§]

[†]International Institute for Carbon-Neutral Energy Research (WPI-I2CNER), [‡]Graduated School of Integrated Frontier Science, Department of Automotive Science, [§]Faculty of Engineering, Department of Applied Chemistry, and [∥]Institute for Materials Chemistry and Engineering, Kyushu University, 744 Motooka, Nishi-ku, Fukuoka 819-0395 Japan

Supporting Information

ABSTRACT: A series of *syn*/*anti* mixtures of anthradifuran (ADF) and substituent compounds were systematically synthesized, and the effect of substitution at the 5,11-positions on the neutral and radical states of ADF was investigated. All compounds were measured and analyzed by absorption and fluorescence spectroscopy, cyclic voltammetry, electrochemical absorption spectroscopy, and DFT calculations. The absorption spectra of 5,11-substituent compounds in their neutral state were red-shifted. In addition, the substituted compounds exhibited increased thermal stability with respect to the parent **1a** because of elongation of the π-conjugation and an increased steric hindrance effect due to the bulky ethynyl substituent groups. The cyclic voltammograms of all of the compounds exhibited irreversible reduction potentials and irreversible oxidation potentials, except in the case of (trimethylsilyl)-silylethynyl-substituted ADF. When the materials were subjected to oxidation/reduction potentials, the radical cation and anion species were generated. The absorption spectra of the radical-cation species of the compounds exhibited similar characteristics and similar absorption ranges (550−1400 nm), whereas the spectra of the radical anion species were blue-shifted (550−850 nm) compared than that of the parent $\mathbf{1a}^{\bullet-}$ (550−1100 nm). The DFT computation results suggested that the radical states of lowest energy transitions occurred primarily from π to π_{SOMO} or from π_{SOMO} to π^*.

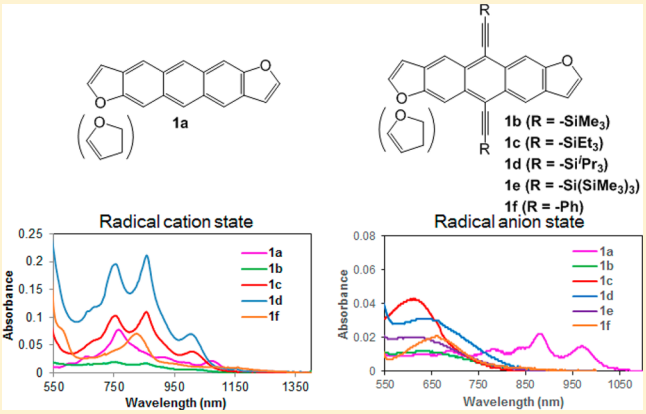

INTRODUCTION

Acenes and acene-related structures have attracted considerable attention as building blocks of semiconducting materials such as organic field-effect transistors (OFETs),[1] organic photovoltaic (OPV) devices,[2] and organic light-emitting diodes (OLEDs)[3a] and transistors (OLETs).[3b−d] A variety of functionalized acene and heteroacene structures have been extensively investigated because these structures are promising materials in the field of optoelectronic materials chemistry. In optoelectronic devices, organic semiconductors can serve as charge-transport materials. For example, alkylthio- or arylthio-substituted pentacene[4] and (trialkylsilyl)ethynyl-substituted pentacene[5] and higher acenes[6,7] have been investigated. Such sterically bulky substituent groups can provide high solubility in solvents and good thermal stability. Typically, silylethynyl-substituted acenes exhibit good charge-transport properties in OFETs,[8] good photoconductivity,[9] and good performance in OPV devices.[10] The thiophene ring-fused acenes such as dithioanthracene,[11] naphthodithiophene,[12] thiotetracene,[13] thiopentacene,[14] and their analogues[15] also exhibit good thermal properties and charge-transport properties when used in OFETs. The compounds used in such applications are required to exhibit good stability and redox properties in solution and/or in the solid state. Although the semiconducting properties of the aforementioned thiophene ring-fused acenes have been investigated extensively, the study of radical species of acene compounds has been sporadic, and the properties of radical species formed by introducing a substituent group have not been examined adequately.[16]

Recently, we investigated the synthesis of triisopropylsilyl (TIPS)-functionalized difuranoacene compounds[17,18] that exhibited high thermal stability in the solution state; these compounds were therefore successfully applied in OFETs,[17] solid-state OPVs,[17] and dye-sensitized solar cells.[19] In the present work, we investigated the effect of substitutions at the 5,11-position on the optoelectrochemical properties and stability of *syn*/*anti* mixtures of difuranoanthracene. The

Received: July 4, 2015
Published: August 24, 2015

ACS Publications © 2015 American Chemical Society

DOI: 10.1021/acs.joc.5b01525
J. Org. Chem. 2015, 80, 9159−9166

compounds exhibited high stability in their neutral state, but their stabilities in the radical cation/anion state differed depending on the substituent group.

RESULTS AND DISCUSSION

Synthesis. Scheme 1 shows the synthesis of anthradifuran (ADF) compounds. Starting material **4** from reacted **2** with **3**

Scheme 1. Synthetic Scheme for the Preparation of Compounds[a]

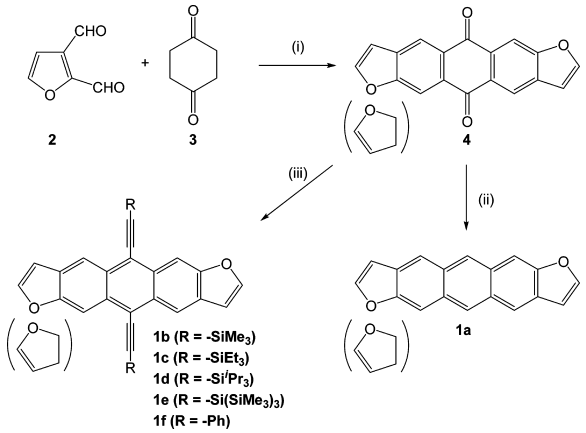

[a]Key: (i) 15% KOH, EtOH solution, EtOH; (ii) Zn, 8 wt % NaOH, aq, 22%; (iii) ethynylbenzene or ethynyltrialkylsilane, *n*-BuLi, *n*-hexane/THF, then $SnCl_2 \cdot H_2O$, 10% HCl aq, 29% for **1b**, 12% for **1e**, 19% for **1f**.

has been reported in the literature.[17] The quinone structure was reduced with activated Zn in 8 wt % NaOH aqueous solution to give a *syn*/*anti* mixture of nonsubstituted **ADF** in 22% yield. Previously, Takimiya et al. reported the synthesis of pure *anti*-**1a**.[11] In this case, the pure *anti*-**1a** exhibited C_{2h} symmetry, generating nine peaks in its ^{13}C NMR spectrum. The ^{13}C NMR spectrum of the *syn*/*anti* mixture of **1a** contained 10 additional peaks that originated from *syn*-**1a**, suggesting that the *syn*/*anti* mixture of **1a** exhibited C_{2v} symmetry. In addition, the structure was confirmed by MALDI-MS spectra for *m*/*z* 258.0678 (M^+, calcd 258.0681 error = −1.0 ppm). In our previous study, we reported that functionalized ethynyl substituents such as an ethynyltriethylsilyl substituent (**1c**) or an ethynyltriisopropylsilyl substituent (**1d**) could be introduced into a quinone moiety (**4**) via a one-pot reaction of an ethynyllithium/tin chloride system.[5,17] A similar synthetic method allowed the introduction of other substituents, e.g., ethynylbenzene (**1f**), ethynyltrimethylsilane (**1b**), and ethynyltris(trimethylsilyl)-silane (**1e**). ^{13}C NMR spectroscopy indicated that of **1b** and **1e** were *syn*/*anti* mixtures. Compound **1f** was not measured by ^{13}C NMR spectroscopy due to its low solubility in solvent; however, we confirmed the *syn*/*anti* mixture structure by X-ray crystallographic analysis study (see the next section). The corresponding ^{13}C NMR indicated almost equal relative intensities for the *syn*/*anti* products, consistent with the results of our previously reported synthesis of higher difranoacenes.[18]

X-ray Crystallographic Study. The structure of **1f** was successfully analyzed by X-ray single-crystallographic analysis (Figure 1). Crystals of **1f** suitable for X-ray diffraction analysis were obtained by slowly evaporating the solvent (toluene). The structure of **1f** was analyzed as a *syn*/*anti* mixture. The structure of **1f** revealed that the plane angle between C6−C5−C7′−C6′−C5′−C7 and C5−C4−C3−C2−C1−O1−C9′−C8′−C7′ was only 2.1° and that the substituent group plane angle between C6−C5−C7′−C6′−C5′−C7 and C12−C13−C14−C15−C16−C17 was 8.6°. These planar structures suggested the π-conjugation was effectively introduced between the ADF core and the phenylethynyl group.

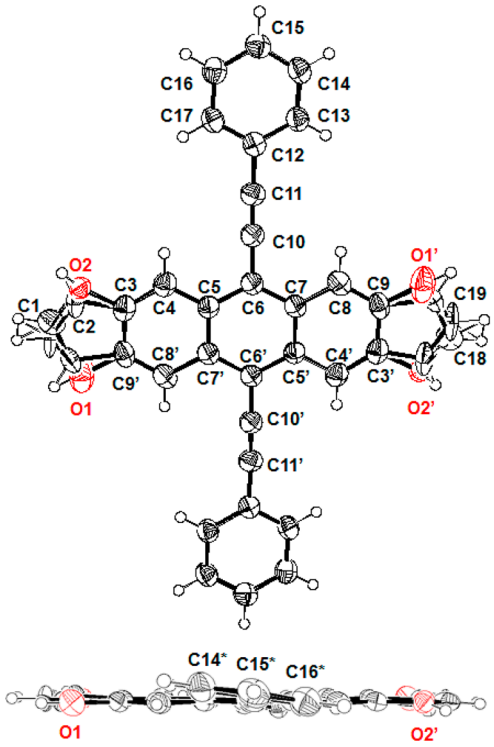

Figure 1. Single crystal structure of **1f** from toluene, with displacement ellipsoids at 50% probability level.

Physical Properties. Absorption Spectra. The absorption spectra of all the compounds in the CH_2Cl_2 solvent (1.0×10^{-6} M) are shown in Figure 2a,b. The spectrum of acene showed three characteristic absorption bands (i.e., ^{1}La, ^{1}Lb, and ^{1}B). The ^{1}La band is polarized along the short axis, and the ^{1}Lb and ^{1}B bands are polarized along the long axis.[20] The spectrum of the parent structure **1a** exhibited characteristic $^1A \rightarrow {}^1$La and $^1A \rightarrow {}^1$Lb transitions with vibronic progressions at 450, 422, 398, 378, and 358 nm and $^1A \rightarrow {}^1$B transitions at 308, 292, and 273 nm. This absorption structure and the position of λ_{max} are consistent with those previously reported for pure *anti*-**1a**, suggesting that the *syn* and *anti* moieties in the difuranoanthracene skeleton exhibit similar electronic properties. The spectra of the substituted compounds showed similar transition characteristics, where the vibration bands were red-shifted to 60−76 nm in the order of increasing absorption coefficients in the range from 529 to 376 nm; i.e., the λ_{max} order was **1f** (529 nm) > **1e** (527 nm) > **1d** (512 nm) = **1c** (512 nm) > **1b** (511 nm). These results are attributed to strong π-delocalizing transition interactions prevalent among the ADF moiety and ethynyl substituents. The higher energy bands in the range from 270 to 310 nm were assigned as $^1A \rightarrow {}^1$B bands, whereas a new band at 338 nm for **1f** was assigned to $\pi-\pi$ conjugation between the **1f** moiety and the ADF backbone. The band at 324 nm in the spectrum of **1e** was due to $\sigma-\pi$ conjugation[21] between the ethynylsilyl moiety and the ADF backbone.

Stability of ADF Derivatives in the Ground State. Compounds **1d** and **1c** have both been reported to exhibit

DOI: 10.1021/acs.joc.5b01525
J. Org. Chem. 2015, 80, 9159−9166

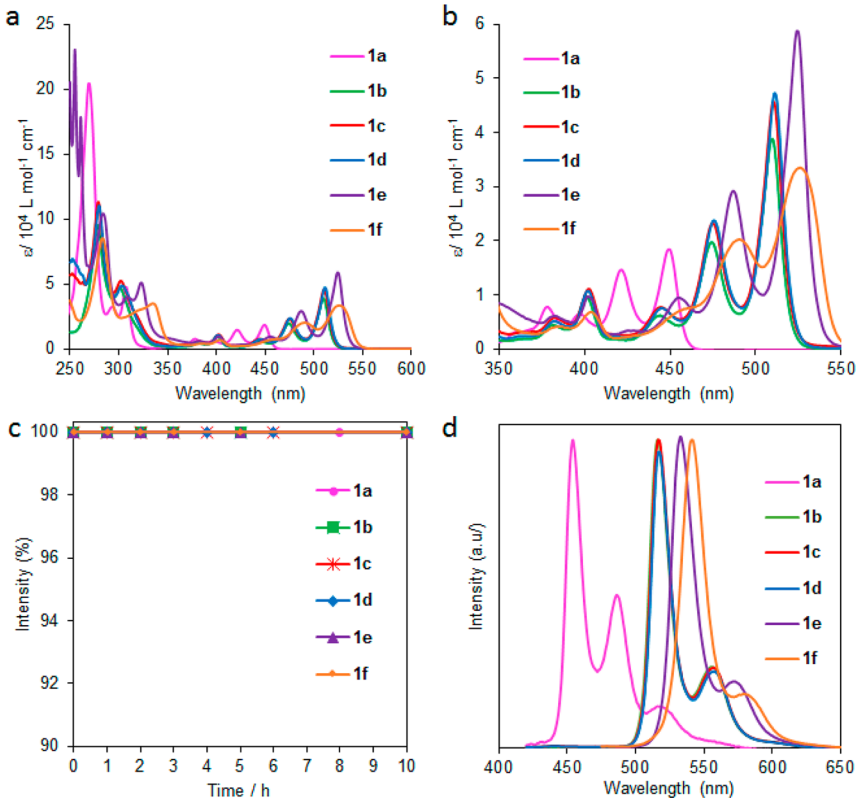

Figure 2. (a) Electronic absorption spectra and (b) an enlarged view at 400−550 nm. (c) Stability of ADFs under ambient conditions (CH_2Cl_2, 1×10^{-6} M). Intensities were counted at the lowest energy of absorption peaks. (d) Fluorescence spectra of compounds (CH_2Cl_2, 1×10^{-6} M).

good stability at ambient condition because their absorption peaks exhibited no change over a 10-h period with the samples exposed to ambient conditions.[17] Other difuranoanthracenes and their derivatives also exhibited good stabilities over a 10-h period under ambient conditions. These results indicate that ADF is extremely thermally stable both in solution state under ambient conditions (Figure 2c). To evaluate the further information for thermal stability, we measured the difference of absorption intensity in toluene at 373 K (sealed tube). The intensity of **1a** at the lowest energy peak disappeared after 12 h, whereas the intensities of the ethynyl substituent groups remained after 12 h: **1e** (100%) > **1d** (90%) > **1e** (80%) > **1c** (69%) = **1b** (69%), suggesting the bulky group increased the thermal stability by avoiding the decomposition pathways such as reaction with dimerization and oxidation[22] (Figure S1).

Fluorescence Spectroscopy. The fluorescence spectra of the difuranoacenes were measured with the samples dissolved in CH_2Cl_2 (1×10^{-6} M, Figure 2d). The wavelength of maximum fluorescence followed the same order as λ_{max} in the absorption spectra: **1f** (541 nm) > **1e** (532 nm) > **1d** (517 nm) = **1c** (517 nm) > **1b** (516 nm) > **1a** (454 nm). The quantum yield was determined in CH_2Cl_2 solution (10^{-6} M) and was calculated relative to the quantum yield of standard compound perylene (Φ = 0.94). All the substituent molecules exhibited higher yields (Φ = 0.34−0.57) than the parent molecule **1a** (Φ = 0.16) because of the change in the electronic structure of ADF. In the trialkylsilyl group, **1b** exhibited the highest value (Φ = 0.57), and the values decreased with increasing bulkiness, i.e., **1b** (0.57) > **1c** (0.45) > **1d** (0.42) > **1e** (0.38). **1f** exhibited the smallest yield among the substituted compounds (Φ = 0.34). These quantum yields were lower than those of TIPS-pentacene (Φ = 0.75) and functionalized TIPS-dithioanthracene (Φ = 0.70−0.76).[8] Although the (trialkylsilyl)ethynyl group exhibited similar absorption and fluorescence character, different quantum yields were observed. These results suggest that the extent of nonrelative fluorescence quenching in the molecules differed.

To verify the component of fluorescence and nonrelative fluorescence kinetics, the fluorescence decay profiles of the samples dissolved in 10^{-6} M CH_2Cl_2 were measured (Figure 3). The fluorescence lifetimes (τ) of all the compounds were analyzed using single-exponential decay profiles, and the radiative (k_r) and nonradiative (k_{nr}) decay rate constants

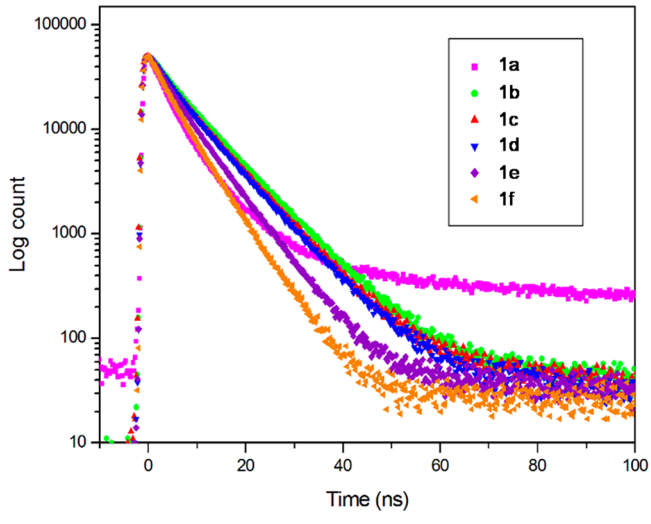

Figure 3. Fluorescence decays of compounds (CH_2Cl_2, 10^{-6} M).

DOI: 10.1021/acs.joc.5b01525
J. Org. Chem. 2015, 80, 9159−9166

were calculated by $k_r = \Phi/\tau$ and $k_{nr} = (1 - \Phi)/k_r$, respectively. In a previous fluorescence study involving acene, the fluorescence lifetime was observed to increase because the electronic structure of anthracene and its derivatives was changed when a polar substituent group was attached to the anthracene skeleton.[25] However, when a similar electron-donating group of an alkyl chain was attached to a tetracene core, almost no change in the fluorescence yield was observed because the alkyl chain hardly affected the electronic properties of tetracene.[26] Although the (trialkylsilyl)ethynyl groups (**1b**, **1c**, and **1d**) exhibited similar absorption spectra and HOMO−LUMO properties, their fluorescence yields were observed to differ. To understand this phenomenon, we tested the fluorescence decay to verify the radiative and nonradiative pathways. The lifetime of the parent **1a** was estimated to be 4.83 ns, whereas the lifetimes of the ethynyl substituent groups increased following a trend similar to that of the quantum yield; the lifetimes were estimated to fall within the range of 5.12−7.96 ns. In the substituted molecules, the k_r and k_{nr} were strongly dependent on the size of the bulky group. In the silylethynyl substituent group, the k_r values decreased and the k_{nr} values increased with increasing size of the bulky group. The phenyl ethynyl group also exhibited a longer decay lifetime and a higher k_r than **1a**; however, the phenyl ethynyl group exhibited the lowest k_r value among the ethynyl-substituted compounds.

Cyclic Voltammetry (CV). In the absorption spectra, changes in the λ_{max} positions due to introduction of the substituents were confirmed (Figure 4). To determine the effects of substituents on the electron-donating and electron-accepting properties of compounds, CV was performed on samples dissolved in CH_2Cl_2 containing 0.1 M n-Bu_4NPF_6 as an electrolyte. When the bias was swept to the negative side, we observed irreversible reduction properties, i.e., in the order **1a** [$E^{red}(I)$: − 2.45 V], **1d** [$E^{red}(I)$: − 1.82 V], **1c** [$E^{red}(I)$: − 1.82 V], **1b** [$E^{red}(I)$: − 1.82 V], **1e** [$E^{red}(I)$: − 1.90 V], and **1f** [$E^{red}(I)$: − 1.79 V, − 2.04 V]. The irreversible oxidation potentials of the compounds tended to follow the same trend with the exception of **1e**: **1a** [$E^{ox}(I)$: + 0.31 V], **1d** [$E^{ox}(I)$: + 0.49 V], **1c** [$E^{ox}(I)$: + 0.49 V], **1b** [$E^{ox}(I)$: + 0.48 V], and **1f** [$E^{ox}(I)$: + 0.41 V]. Compared with the parent compound **1a**, the reduction potential and HOMO−LUMO gap of all the ethynyl-substituted compounds were positively shifted and narrower, respectively, suggesting that the ethynyl groups of **ADF** elongated the electronic π-conjugation. Among the silylethynyl group of compounds, **1b**, **1c**, and **1d** showed similar reduction and oxidation potentials, indicating weak electronic interactions between the alkyl and silyl groups. In contrast, **1e** and **1f** exhibited much narrower HOMO−LUMO gaps, suggesting π-elongated conjugations between the phenyl and acetylene groups and the presence of $\sigma-\pi$ interactions between the (trimethylsilyl)silsyl group and acetylene moiety. Compound **1f** showed decoalescence of reduction potential due to this π-elongated conjugation. This π-elongated conjugation between the phenyl and ADF skeleton over acetylene groups was confirmed by DFT computations (see the discussion on DFT computations). The oxidation and reduction potentials of the gaps agreed well with the order of the 0−0 band gaps determined from the absorption and fluorescence spectra. Compound **1e** did not exhibit a reversible oxidation potential, possibly because of electrochemical decomposition of the **1e** moiety. The data are summarized in Table 1.

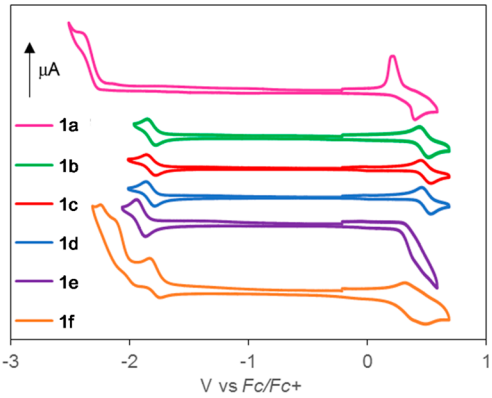

Figure 4. Cyclic voltammogrums of compounds in CH_2Cl_2 solution with n-Bu_4NPF_6 as supporting electrolyte. The measurement was performed under Ar atmosphere; scan rate 200 mV/s.

Electrochemical Properties. In organic material based devices such as OFETs, OPVs, DSSCs, and OLEDs, acene compounds serve as the hole or electron injection/transport layer. During hole or electron injection/transport, important reactions occur between the neutral state and radical cation/anion states. The electrochemical spectra of difuranoacenes in the monoradical cation state were investigated in CH_2Cl_2 solutions containing 0.1 M n-Bu_4NPF_6 (Figure 5a,b). When a bias was applied at the oxidation potentials for these compounds, new peaks were generated at 550−1400 nm. The parent structure of **1a** exhibited peaks between 550 and 1200 nm, including four characteristic peaks at 1071, 905, 765, and 660 (sh) nm. Relative to the λ_{max} of the neutral state, the lowest λ_{max} peak was red-shifted to 621 nm. The spectra of the (trialkylsilyl)ethynyl-substituted compounds were similar, with similar peak positions between 650 and 1100 nm. The structures of these compounds in their radical-cation states were similar to those of the compounds in their neutral states, suggesting similar delocalization of molecular orbitals and similar transitions in ADF cores. Compound **1f** exhibited a

Table 1. Experimental Results of Absorption Spectra, Cyclic Voltammetry, Fluorescence Spectra, and Decay Life Time

	experimental					
compd	wavelength (nm/M^{-1} cm^{-1})	HOMO/LUMO (V vs Fc/Fc^+)	FL (nm)	FL (Φ)	τ (ns)	k_r/k_{nr} (10^{-7}/s)
1a	451/10000	+0.31/−2.45	454, 486, 516	0.16	4.83	3.22/17.48
1b	511/38000	+0.48/−1.82	516, 556	0.57	7.96	7.14/5.42
1c	512/44000	+0.49/−1.82	517, 557	0.45	7.51	5.98/7.34
1d	512/46000	+0.49/−1.82	517, 557	0.42	7.22	5.77/8.08
1e	527/53000	−/−1.90	532, 571	0.38	6.08	6.32/10.12
1f	529/42000	+0.41/−1.79, −2.04	541, 579	0.34	5.12	6.57/12.97

DOI: 10.1021/acs.joc.5b01525
J. Org. Chem. 2015, 80, 9159−9166

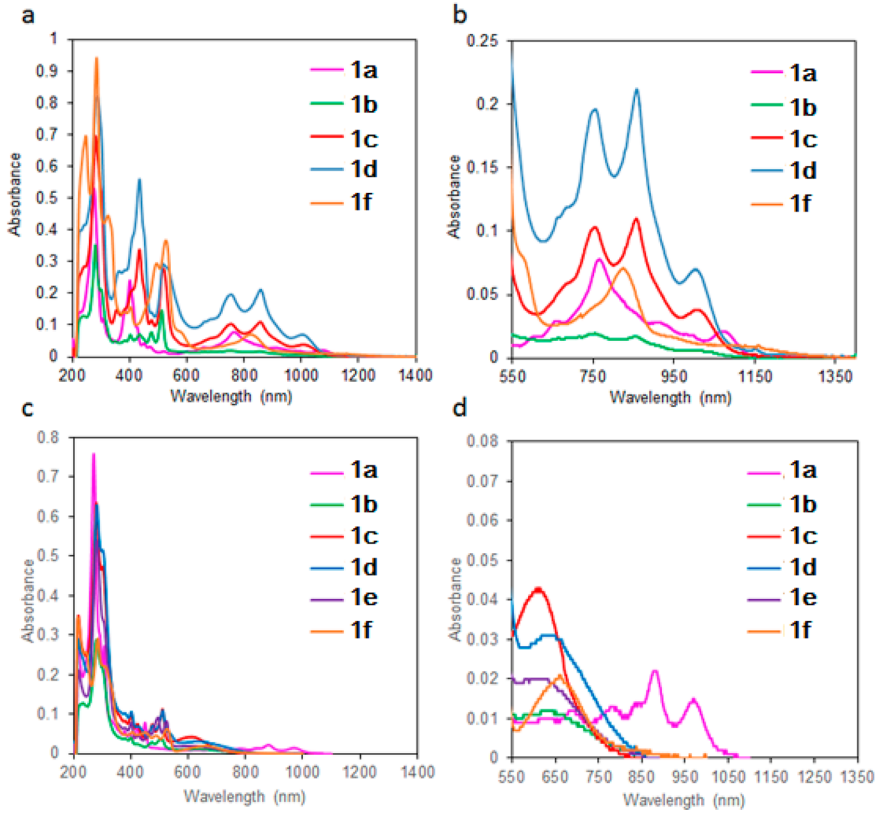

Figure 5. Electrochemical absorption spectra of compounds: (a) radical cation state of absorption spectra and (b) enlarged spectra of (a). 0.1 mM of compounds in CH_2Cl_2 solution with 0.1 M Bu_4NPF_6 as supporting electrolyte. (c) Radical anion state of absorption spectra and (d) enlarged spectra of (a). Compounds (0.1 M) in THF solution with 0.1 M Bu_4NClO_4 as supporting electrolyte. Each reaction was given the redox potentials of these compounds. The measurement were accomplished in Ar flow atmospheres at 298 K.

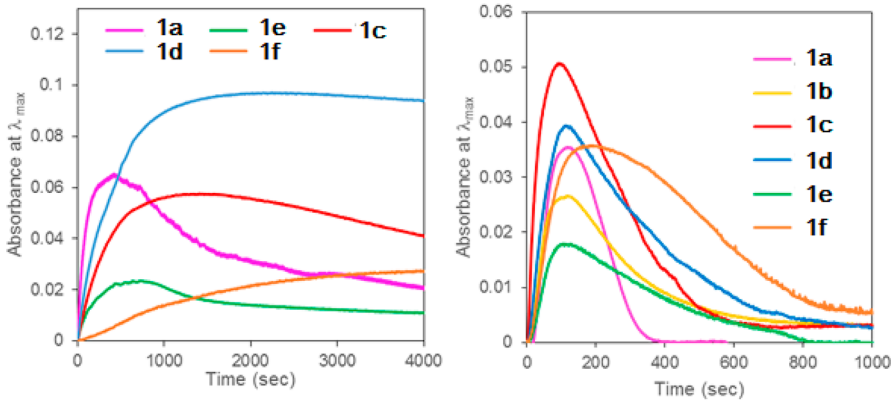

Figure 6. Stationary time course measurement (lowest energy of λ_{max}) of compounds at different electrochemical reaction times. (Left) Radical cation species, 0.1 mM of compounds in CH_2Cl_2 solution with 0.1 M Bu_4NPF_6 as supporting electrolyte. (Right) Radical anion species, 0.1 mM of compounds in THF solution with 0.1 M Bu_4NClO_4 as supporting electrolyte. Each reaction was given the redox potential of these compounds. The measurements were accomplished in Ar flow atmospheres at 298 K.

much bolder structure than the parent **1a**, and the lowest energy band was elongated to approximately 1400 nm. This suggested that the radical-cation states of the orbitals of the phenyl groups were delocalized because of phenyl group rotation at the radical cation state. No characteristic peaks were observed for **1e**, supporting our previous deduction based on the cyclic voltammograms that the radical-cation state of this compound is not stable.

The radical anion spectra of samples were performed with 0.1 mM of compounds in THF solution in the presence of 0.1 M Bu_4NClO_4 as supporting electrolyte (Figure 5c,d). The radical anion of **1a** showed new absorption bands around 550–1100 nm, with characteristic new peaks at 970, 881, 846, 781, 688, and 630 nm, respectively. The absorption of the radical anion state of the ethynyl substituent groups was observed around 550–850 nm. All of the peaks were much broader with a blue shift compared with the parent **1a** and the respective radical cations.

Stability of Radical Species. To investigate the effect of substituents on the stability of radical states, we performed time-dependent measurements of radical species (Figure 6). Measured potentials were used as these compounds' redox

DOI: 10.1021/acs.joc.5b01525
J. Org. Chem. 2015, 80, 9159–9166

potentials, and in situ time-course measurements were performed for this study. The radical cation of **1a**, $\mathbf{1a}^{\bullet+}$, was immediately generated when the bias was applied. The half-life of the radical cation of **1a** was estimated to be 916 s under these conditions. The silylethynyl substituents of radical-cation species also immediately formed after a given bias was applied, whereas these species persisted much longer than any substituent of ADF. The half-lives of the radical-cation species under the conditions used in this study were estimated to be 1332, 6097, and >41700 s in the case of **1b**, **1c**, and **1d**, respectively. However, in the case of **1f**, the radical-cation species was gradually generated and exhibited a longer half-life than the radical-cation species of the parent **1a** and **1d** compounds. The radical-anion species exhibited phenomena similar to those of the radical-cation species; however, the half-lives of these species were much smaller (121−402 s) than those of the radical cations. Although the radical-cation species of **1e** could not be measured, the stabilities of both radical species were evident in the differences among substituent groups, whose stabilities decreased in the order **1f** > **1e** > **1d** > **1c** > **1b** > **1a**. This result suggests that the structure of bulky substituents could protect the ADF core in the radical state and that this effect may reduce the unfavorable dimerization reaction and reactions with other species such as solvent molecules and electrolyte species.

To gain insight into the electronic properties of compounds, DFT and TD-DFT computations of neutral, radical cation, and anion states were performed. All of the structures were calculated as *anti* structures. The optimized structures were calculated at the B3LYP/6-31+G(d) and the UB3LYP/6-31+G(d)level for neutral and radical structures, and TD-DFT computations were evaluated at the B3LYP/6-311+G(d,p) and the UB3LYP/6-311+G(d,p) levels for neutral and radical structures. In the case of their neutral states, all molecules exhibited HOMO−LUMO transitions. The HOMO and LUMO for **1a** were delocalized on the ADF core, which suggested a $\pi-\pi^*$-type transition. TD-DFT study of pentacene and **1d** pentacene revealed that the effect of the ethynyl moiety was to expand the delocalization of MO to the triple bond of the **1d** group, which reduced the HOMO−LUMO band gap because of a shift of the ionization potential and electron affinity.[23] When an ethynyl group was attached at the 5,11-position of ADF, all ethynyl-substituted compounds of the delocalized orbitals were extended to the C≡C triple bond of the ethynyl group. The HOMO−LUMO gaps were reduced when the LUMOs were comparatively shifted to higher potentials, whereas the HOMOs remained almost unchanged. In the case of **1f**, efficient $\pi-\pi^*$ orbital interaction was observed to extend to the phenyl group as the HOMO−LUMO gap decreased (Table 2). Decoalescence of reduction potentials is discussed in the Cyclic Voltammetry section. DFT computation results of the molecular orbitals (MOs), except for **1f**, were delocalized to the ethynylsilyl moieties of the C≡C bond on the ADF skeleton at LUMO and LUMO+1, while **1f** showed delocalized the orbitals on a phenyl group over acethylene moieties int he ADF skeleton. Therefore, this effective $\pi-\pi^*$ orbital interaction caused decoalescence of reduction potentials.

Table 2. TDDFT Results of Compounds at Neutral State

	computational			
compd	wavelength (nm)	oscillator strength (f)	HOMO/LUMO (eV)	transition/ density
1a	479	0.0864	−5.12/−2.22	H → L
1b	555	0.2607	−5.13/−2.66	H → L
1c	557	0.2782	−5.12/−2.66	H → L
1d	558	0.3066	−5.12/−2.66	H → L
1e	573	0.4190	−4.98/−2.57	H → L
1f	595	0.5305	−5.02/−2.74	H → L

The main electronic transition of the radical state at doublet states can be divided into two types. One involves promotion of an electron from a SOMO to a higher unoccupied orbitals; the other type is electron promotion to a SOMO from a lower, doubly occupied orbital.[24] TD-DFT calculations were performed for both the radical anion and cation states. Although radical states of **1a** appeared to absorb shorter wavelengths as DFT results compared with other compounds, the characteristics of the absorption bands of other groups of compounds were generally consistent. As mentioned in the discussion of the calculation results, the major transitions of the radical cation and anion states, the parent **1a**, and ethynyl-substituted ADFs differed. In its radical cation state, **1a** exhibited a major transition from SOMO-1 (β) to SOMO (β), whereas other compounds in their radical cation states appeared to exhibit transitions from SOMO (α) to LUMO (α). However, the radical anion state of **1a** exhibited a transition from SOMO (α) to LUMO (α), whereas the others exhibited a transition from SOMO-1 (β) to SOMO (β). Both states of orbitals were delocalized on the ADF core in the case of **1a** and on the ADF core over the triple bond of the ethynyl group (phenyl group for **1f**) in the case of ethynyl-substituted ADFs. These results suggest that the characters of the first excitation types for radical cation states are $\pi-\pi_{SOMO}$ for **1a** and $\pi_{SOMO}-\pi^*$ for ethynyl-substituted ADFs, whereas the radical anion states are $\pi_{SOMO}-\pi^*$ for **1a** and $\pi-\pi_{SOMO}$ for ethynyl-substituted ADFs, respectively (Figure 7 and Table 3).

CONCLUSION

In conclusion, we have investigated the neutral and radical cation/anion states of a *syn*/*anti* mixture of **1a** and related compounds substituted at the 5,11-position with an ethynyl

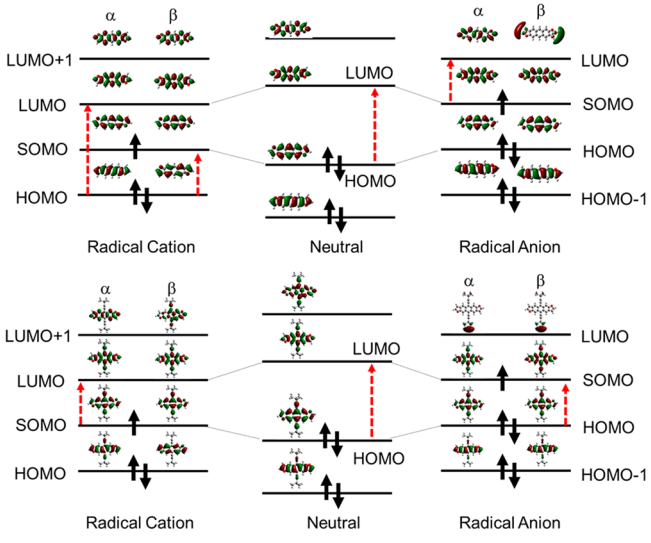

Figure 7. Molecular orbitals and the major transitions of the neutral, radical cation, and anion states for (top) **1a** and (bottom) **1b**.

DOI: 10.1021/acs.joc.5b01525
J. Org. Chem. 2015, 80, 9159−9166

Table 3. Characteristic Absorption Peaks at Radical State and Theoretical Results

	experimental		theoretical	
compd	wavelength (nm)	$\tau_{1/2}$ (s)	wavelength (nm)/f	character
$\mathbf{1a}^{\bullet+}$	1071, 905, 765, 660	916	763/0.1198	H(β) → S(β) H(α) → L(α)
$\mathbf{1b}^{\bullet+}$	1001, 853, 754, 688	1332	797/0.0622	S(α) → L(α) H(β) → S(β)
$\mathbf{1c}^{\bullet+}$	1007, 857, 754, 686	6097	802/0.0596	S(α) → L(α) H(β) → S(β)
$\mathbf{1d}^{\bullet+}$	1004, 858, 755, 688	>41700	809/0.0483	S(α) → L(α) H-1(β) →S(β)
$\mathbf{1e}^{\bullet+}$				
$\mathbf{1f}^{\bullet+}$	1159, 946, 824	>41700	896/0.0284	S(α) → L(α) H-1(β) → S(β)
$\mathbf{1a}^{\bullet-}$	970, 881, 846, 781, 688, 630	121	782/0.2514	S(α) → L(α) H(β) → S(β) H-1(β) → S(β)
$\mathbf{1b}^{\bullet-}$	631	191	807/0.1159	H(β) → S(β)
$\mathbf{1c}^{\bullet-}$	615	203	809/0.1217	H(β) → S(β)
$\mathbf{1d}^{\bullet-}$	635	253	810/0.1315	H(β) → S(β)
$\mathbf{1e}^{\bullet-}$	611	271	822/0.1658	H(β) → S(β)
$\mathbf{1f}^{\bullet-}$	660	402	911/0.0566	H(β) → S(β) S(α) → L + 1(α)

group in solution state. To investigate the effect of the ethynyl group in solution state, the unsubstituted structure of **1a** and a variety of ethynyl-substituted compounds **1b**, **1e**, and **1f** were synthesized. All of the compounds were confirmed as mixtures of *syn*/*anti* structures by ^{13}C NMR or single-crystal X-ray crystallographic analysis. The parent structure of the *syn*/*anti* mixture, ADF, exhibited an absorption spectrum and cyclic voltammogram similar to those reported for pure *anti*-**1a**, suggesting that the *syn* and *anti* structures exhibit similar physical properties. The absorption spectra of all the ground-state compounds in the solution state under ambient condition did not change, suggesting that the ADF structure and substituted moieties are highly stable. According to the fluorescence lifetimes and quantum efficiencies of **1a** and its ethynyl-substituted analogues, the ethynyl group enhanced the fluorescence lifetime and radiative quenching; however, sterically larger substituents favored nonradiative quenching. The fluorescence spectra of the radical cation and anion states exhibited new peaks at 550−1400 nm for the radical cation state and at 550−1100 nm for the radical anion state, respectively. The stabilities of both radical states increased with increasing size of the substituent group in the alkylsilyl moieties. DFT computation results showed that the $\pi_{SOMO}-\pi^*$ and $\pi-\pi_{SOMO}$ transitions were the primary contributors to the radical state of the first excitation.

EXPERIMENTAL SECTION

***cis*- and *trans*-Anthradifuran (1a).** To a mixture of quinone **4** (500 mg, 1.74 mmol) and 8 wt % NaOH aq (35 mL) was added activated zinc (4 g), and the mixture was refluxed for 36 h in Ar atmosphere. After completion of the reaction, the mixture was cooled in an ice bath, and then concd HCl (100 mL) was added. The suspension was extracted with 500 mL of toluene, washed with water, and dried with anhyd $MgSO_4$. The solvent was evaporated to ca. 50 mL, and the precipitate was filtrated to give pure **1a** (97 mg, 22%).

Physical data of ***1a:*** yellow solid; mp 286−288 °C (subl); δ_H (THF-d_6, 600 MHz) 6.92−6.93 (m, 2H), 7.84−7.85 (m, 2H), 8.03−8.04 (m, 2H), 8.23−8.24 (m, 2H), 8.67−8.74 (m, 2H); δ_C (THF-d_6, 150 MHz) 105.5, 105.8, 106.9, 106.9, 118.9, 119.3, 125.7, 126.4, 127.0, 129.7, 130.2, 130.3, 130.4, 130.7, 130.8, 149.5, 149.6, 154.6, 154.9; HRMS (FAB) m/z $[M]^+$ calcd for $C_{18}H_{10}O_2$ 258.0681, found 258.0678). Anal. Calcd for $C_{18}H_{10}O_2$: C, 83.71; H, 3.90. Found: C, 83.65; H, 3.83.

***cis*- and *trans*-5,11-Bis((trimethylsilyl)ethynyl)anthradifuran (1b).** To a mixture of (trimethylsilyl)acetylene (0.96 g) and dried hexane (20 mL) was slowly added *n*-BuLi (4.3 mL, 6.87 mmol, 1.6 mol/L in hexane) at −5 °C in Ar atmosphere. After additional reaction at −5 °C for 30 min, the reaction mixture was allowed to react at rt for an additional 1 h. To the mixture were added **4** (300 mg, 1.04 mmol), dry hexane (200 mL), and THF (5 mL), and then the mixture was stirred at rt overnight. To the mixture were added $SnCl_2{\cdot}H_2O$ (1.5 g, 6.64 mmol) and 10% HCl aq (5.4 mL), and the mixture was stirred at rt for 2 h. After the reaction, the mixture was extracted with $CHCl_3$, washed with brine, and then dried with anhyd $MgSO_4$. Silica gel chromatography with CH_2Cl_2/hexane gave **1b** (126 mg, 29%).

Physical data of ***1b:*** orange solid; mp 288−290 °C dec; δ_H ($CDCl_3$, 600 MHz) δ = 0.48 (t, J = 3.15 Hz, 18H), 6.96−6.97 (m, 2H), 7.77−7.78 (m, 2H), 8.64 (s, 1H), 8.65 (s, 1H), 8.81 (s, 1H), 8.83 (s, 1H); δ_C ($CDCl_3$, 150 MHz) δ = 0.3, 102.4, 102.6, 102.8, 105.3, 105.5, 106.6, 106.6, 108.1 108.3, 108.4, 117.4, 117.7, 118.1, 118.4, 129.1, 129.5, 130.1, 130.2, 130.4, 130.6, 148.8, 148.9, 154.6, 154.7; HRMS (FAB) m/z $[M]^+$ calcd for $C_{28}H_{26}O_2Si_2$ 450.1471, found 450.1472. Anal. Calcd for $C_{28}H_{26}O_2Si_2$: C, 74.62; H, 5.82. Found: C, 74.66; H, 5.80

***cis*- and *trans*-5,11-Bis(tris(trimethylsilyl)silylethynyl)-anthradifuran (1e).** To a mixture of tris(trimethylsilyl)silylacetylene (2.27 g) and dried hexane (20 mL) was added *n*-BuLi (3.9 mL, 6.22 mmol, 1.6 mol/L in hexane) slowly at −5 °C in Ar atmosphere. After additional reaction at −5 °C for 30 min, the reaction mixture was allowed to react at rt for an additional 1 h. To the mixture were added **4** (270 mg, 0.94 mmol), dry hexane (200 mL), and dried THF (5 mL), and then the mixture was stirred at rt overnight. To the mixture were added $SnCl_2{\cdot}H_2O$ (1.5 g, 6.64 mmol) and 10% HCl aq (5.4 mL), and the mixture was stirred at rt for 2 h. After the reaction, the mixture was extracted with $CHCl_3$, washed with brine, and then dried with anhyd $MgSO_4$. Silica gel chromatography with CH_2Cl_2/hexane gave **1e** (104 mg, 12%).

Physical data of ***1e:*** red solid; mp >300 °C; δ_H ($CDCl_3$, 600 MHz) δ = 0.39 (s, 54H), 6.88 (s, sH), 7.76 (s, 2H), 8.64 (s, 1H), 8.65 (s, 1H), 8.85 (s, 1H), 8.86 (s, 1H); δ_C ($CDCl_3$, 150 MHz) δ_C = 0.9, 103.0, 103.2, 103.5, 105.6, 105.8, 106.3, 106.5, 106.71, 106.74, 118.1, 118.58, 118.60, 118.8, 119.1, 129.4, 129.9, 130.1, 130.3, 130.4, 130.9, 148.8, 148.9, 154.7, 154.9; HRMS (FAB) m/z $[M]^+$ calcd for $C_{40}H_{62}O_2Si_8$ 798.2904, found 798.2907. Anal. Calcd for $C_{40}H_{62}O_2Si_8$: C, 60.08; H, 7.82. Found: C, 59.73; H, 7.83

***cis*- and *trans*-5,11-Bis((phynyl)ethynyl)anthradifuran (1f).** To a mixture of phenylacetylene (447 mg) and dried THF (10 mL) was added *n*-BuLi (3.83 mL, 6.12 mmol, 1.6 mol/L in hexane) slowly at −78 °C in Ar atmosphere. After additional reaction at −78 °C for 30 min, the reaction mixture was allowed react at rt for an additional 1 h. To the mixture was added **4** (362 mg, 1.25 mmol), then the mixture was stirred at rt overnight. To the mixture were added $SnCl_2{\cdot}H_2O$ (1.5 g, 6.64 mmol) and 10% HCl aq (5.4 mL), and the mixture was stirred at rt for 2 h. After the reaction, the mixture was a crystalline solid which was extracted with $CHCl_3$, washed with brine, and then dried with anhyd $MgSO_4$. Silica gel chromatography with CH_2Cl_2/hexane gave **1f** (108 mg, 19%).

Physical data of ***1f:*** purple-red solid; mp >300 °C; δ_H ($CDCl_3$, 600 MHz) δ = 6.99 (s, 2H), 7.42−7.53 (m, 6H), 7.80 (s, 2H), 7.85 (s, 1H), 8.86 (s, 1H), 8.77 (s, 1H), 8.78 (s, 1H), 8.95 (s, 1H), 8.96 (s, 1H); HRMS (FAB) m/z $[M]^+$ calcd for $C_{34}H_{18}O_2$ 458.1307, found 458.1296. Anal. Calcd for $C_{34}H_{18}O_2{\cdot}0.05CH_2Cl_2$: C, 88.38; H, 3.86. Found: C, 88.49; H, 3.86.

Crystallographic data of the structures reported in this paper have been deposited with the Cambridge Crystallographic Data Centre as supplementary publication CCDC 1409622 (**1f**). Copies of the data can be obtained free of charge on application to CCDC, 12 Union

DOI: 10.1021/acs.joc.5b01525
J. Org. Chem. 2015, 80, 9159−9166

Road, Cambridge CB2 1EZ, UK (Fax: + 44 1223 336 033; e-mail: deposit@ccdc.cam.ac.uk).

■ ASSOCIATED CONTENT

Supporting Information

The Supporting Information is available free of charge on the ACS Publications website at DOI: 10.1021/acs.joc.5b01525.

Experimental details, X-ray diffraction analysis of **1f**, NMR spectra, and DFT results(PDF)

Crystallographic data for **1f** (CIF)

■ AUTHOR INFORMATION

Corresponding Authors

*E-mail: mwata@i2cner.kyushu-u.ac.jp.

*E-mail: ishihara@cstf.kyushu-u.ac.jp.

Notes

The authors declare no competing financial interest.

■ ACKNOWLEDGMENTS

This work was supported by a Grant-in-Aid for Science Research (YB 26810107) from the Ministry of Education, Culture, Sports, Science and Technology (MEXT), Japan, and the Kurata Memorial Hitachi Science and Technology Foundation and was performed under the Cooperative Research Program of "Network Joint Research Centre for Materials and Devices (IMCE, Kyushu University)". M.W. and A.T.S. acknowledge support from I^2CNER, funded by the World Premier International Research Centre Initiative (WPI) and Competitive Funding Initiative Interdisciplinary Research, Ministry of Education, Culture, Sports, Science and Technology of Japan (MEXT), Japan. The computations were carried out using the computer facilities at the Research Institute for Information Technology, Kyushu University.

■ REFERENCES

(1) *Organic Field-Effect Transistors*; Bao, Z., Locklin, J., Eds.; CRC Press: Boca Raton, 2007.

(2) *Organic Photovoltaics: Materials, Device Physics, and Manufacturing Technologies*; Brabec, C., Ullrich Scherf, U., Dyakonov, V., Eds; Wiley-VCH: Weinheim, 2014.

(3) (a) Shao, Y.; Yang, Y. *Appl. Phys. Lett.* **2005**, *86*, 073510. (b) Santato, C.; Cicoira, F.; Cosseddu, P.; Bonfiglio, A.; Bellutti, P.; Muccini, M.; Zamboni, R.; Rosei, F.; Mantoux, A.; Doppelt, P. *Appl. Phys. Lett.* **2006**, *88*, 163511. (c) Santato, C.; Capelli, R.; Loi, M. A.; Murgia, M.; Cicoira, F.; Roy, V. A. L.; Stallinga, P.; Zamboni, R.; Rost, C.; Karg, S. F.; Muccini, M. *Synth. Met.* **2004**, *146*, 329–334. (d) Takahashi, T.; Takenobu, T.; Takeya, J.; Iwasa, Y. *Adv. Funct. Mater.* **2007**, *17*, 1623–1628. (e) Dadvand, A.; Sun, W.-H.; Moiseev, A. G.; Bélanger-Gariépy, F.; Rosei, F.; Meng, H.; Perepichka, D. F. *J. Mater. Chem. C* **2013**, *1*, 2817–2825.

(4) Kaur, I.; Jia, W.; Kopreski, R. P.; Selvarasah, S.; Dokmeci, M. R.; Pramanik, C.; McGruer, N. E.; Miller, G. P. *J. Am. Chem. Soc.* **2008**, *130*, 16274–16286.

(5) (a) Anthony, J. E.; Brooks, J. S.; Eaton, D. L.; Parkin, S. R. *J. Am. Chem. Soc.* **2001**, *123*, 9482–9483. (b) Anthony, J. E.; Eaton, D. L.; Parkin, S. R. *Org. Lett.* **2002**, *4*, 15–18.

(6) (a) Kaur, I.; Stein, N. N.; Kopreski, R. P.; Miller, G. P. *J. Am. Chem. Soc.* **2009**, *131*, 3424–3425. (b) Kaur, I.; Jazdzyk, M.; Stein, N. N.; Prusevich, P.; Miller, G. P. *J. Am. Chem. Soc.* **2010**, *132*, 1261–1263.

(7) (a) Payne, M. M.; Parkin, S. R.; Anthony, J. E. *J. Am. Chem. Soc.* **2005**, *127*, 8028–8029. (b) Purushothaman, B.; Bruzek, M.; Parkin, S.; Miller, A.; Anthony, J. *Angew. Chem., Int. Ed.* **2011**, *50*, 7013–7017. (c) Purushothaman, B.; Parkin, S. R.; Kendrick, M. J.; David, D.; Ward, J. W.; Yu, L.; Stingelin, N.; Jurchescu, O. D.; Ostroverkhova, O.; Anthony, J. E. *Chem. Commun.* **2012**, *48*, 8261–8263.

(8) (A) Giri, G.; Verploegen, E.; Mannsfeld, S. C. B.; Atahan-Evrenk, S.; Kim, D. H.; Lee, S. Y.; Becerril, H. A.; Aspuru-Guzik, A.; Toney, M. F.; Bao, Z. *Nature* **2011**, *480*, 504–508. (b) Kim, D. H.; Lee, D. Y.; Lee, H. S.; Lee, W. H.; Kim, Y. H.; Han, J. I.; Cho, K. *Adv. Mater.* **2007**, *19*, 678–682. (c) Hamilton, R.; Smith, J.; Ogier, S.; Heeney, M.; Anthony, J. E.; McCulloch, I.; Veres, J.; Bradley, D. D. C.; Anthopoulos, T. D. *Adv. Mater.* **2009**, *21*, 1166–1171.

(9) (a) Ostroverkhova, O.; Shcherbyna, S.; Cooke, D. G.; Egerton, R. F.; Hegmann, F. A.; Tykwinski, R. R.; Parkin, S. R.; Anthony, J. E. *J. Appl. Phys.* **2005**, *98*, 033701. (b) Platt, A. D.; Day, J.; Subramanian, S.; Anthony, J. E.; Ostroverkhova, O. *J. Phys. Chem. C* **2009**, *113*, 14006.

(10) Lloyd, M. T.; Anthony, J. E.; Malliaras, G. G. *Mater. Today* **2007**, *10*, 34–41.

(11) Nakano, M.; Niimi, K.; Miyazaki, E.; Osaka, I.; Takimiya, K. *J. Org. Chem.* **2012**, *77*, 8099–8111.

(12) (a) Takimiya, K.; Kunugi, Y.; Toyoshima, Y.; Otsubo, T. *J. Am. Chem. Soc.* **2005**, *127*, 3605–12. (b) Shinamura, S.; Miyazaki, E.; Takimiya, K. *J. Org. Chem.* **2010**, *75*, 1228–34.

(13) Tang, M. L.; Okamoto, T.; Bao, Z. *J. Am. Chem. Soc.* **2006**, *128*, 16002–16003.

(14) Tang, M. L.; Mannsfeld, S. C. B.; Sun, Y.-S.; Becerril, H. A.; Bao, Z. *J. Am. Chem. Soc.* **2009**, *131*, 882–3.

(15) (a) Takimiya, K.; Ebata, H.; Sakamoto, K.; Izawa, T.; Otsubo, T.; Kunugi, Y. *J. Am. Chem. Soc.* **2006**, *128*, 12604–5. (b) Yamamoto, T.; Takimiya, K. *J. Am. Chem. Soc.* **2007**, *129*, 2224–5. (c) Osaka, I.; Abe, T.; Shinamura, S.; Miyazaki, E.; Takimiya, K. *J. Am. Chem. Soc.* **2010**, *132*, 5000–5001. (d) Niimi, K.; Shinamura, S.; Osaka, I.; Miyazaki, E.; Takimiya, K. *J. Am. Chem. Soc.* **2011**, *133*, 8732–8739. (e) Fukutomi, Y.; Nakano, M.; Hu, J.-Y.; Osaka, I.; Takimiya, K. *J. Am. Chem. Soc.* **2013**, *135*, 11445–11448.

(16) Sakanoue, T.; Sirringhaus, H. *Nat. Mater.* **2010**, *9*, 736–740.

(17) Watanabe, M.; Su, W.-T.; Chang, Y. J.; Chao, T.-H.; Wen, Y.-S.; Chow, T. J. *Chem. - Asian J.* **2013**, *8*, 60–64.

(18) Watanabe, M.; Chien, C.-T.; Lin, Y.-D.; Chang, Y. J.; Wen, Y.-S.; Goto, K.; Shibahara, M.; Shinmyozu, T.; Chow, T. J. *Tetrahedron Lett.* **2014**, *55*, 1424–1427.

(19) Lin, Y.-Z.; Yeh, C.-W.; Chou, P.-T.; Watanabe, M.; Chang, Y.-H.; Chang, Y. J.; Chow, T. J. *Dyes Pigm.* **2014**, *109*, 81–89.

(20) Klevens, H. B.; Platt, J. R. *J. Chem. Phys.* **1949**, *17*, 470.

(21) Shimizu, M.; Tatsumi, H.; Mochida, K.; Hiyama, T. *Chem. Commun.* **2008**, 2134–2136.

(22) Maliakal, A.; Raghavachari, K.; Katz, H.; Chandross, E.; Siegrist, T. *Chem. Mater.* **2004**, *16*, 4980–4986.

(23) Malloci, G.; Cappellini, G.; Mulas, G.; Mattoni, A. *Thin Solid Films* **2013**, *543*, 32–34.

(24) Honda, Y.; Shida, T.; Nakatsuji, H. *J. Phys. Chem. A* **2012**, *116*, 11833–11845.

(25) (a) King, L. A. *J. Chem. Soc., Perkin Trans. 2* **1976**, 1725–1728. (b) King, L. A. *J. Chem. Soc., Perkin Trans. 2* **1977**, 919–920.

(26) (a) Kitamura, C.; Ohara, T.; Kawatsuki, N.; Yoneda, A.; Kobayashi, T.; Naito, H.; Komatsu, T.; Kitamura, T. *CrystEngComm* **2007**, *9*, 644–647. (b) Kitamura, C.; Abe, Y.; Ohara, T.; Yoneda, A.; Kawase, T.; Kobayashi, T.; Naito, H.; Komatsu, T. *Chem. - Eur. J.* **2010**, *16*, 890–898. (c) Kitamura, C.; Matsumoto, C.; Yoneda, A.; Kobayashi, T.; Naito, H.; Komatsu, T. *Eur. J. Org. Chem.* **2010**, *2010*, 2571–2575. (d) Kitamura, C.; Tsukuda, H.; Yoneda, A.; Kawase, T.; Kobayashi, T.; Naito, H. *Eur. J. Org. Chem.* **2010**, *2010*, 3033–3040. (e) Kitamura, C.; Ohara, T.; Yoneda, A.; Kawase, T.; Kobayashi, T.; Naito, H. *Chem. Lett.* **2011**, *40*, 58–59.

DOI: 10.1021/acs.joc.5b01525
J. Org. Chem. 2015, 80, 9159–9166